Nonparabolicity effects in a quantum well: Sublevel shift, parallel mass, and Landau levels

U. Ekenberg
Cavendish Laboratory, Madingley Road, Cambridge CB3 0HE, United Kingdom
*and Department of Physics, Uppsala University, P.O. Box 530, S-751 21 Uppsala, Sweden**
(Received 29 November 1988; revised manuscript received 19 June 1989)

The influence of nonparabolicity on the subband structure in a quantum well is analyzed. Starting from an accurate expression for the bulk conduction-band structure expanded up to fourth order in k, we determine both the shift of the confinement energies and the energy dispersion parallel to the layers $E(\mathbf{k}_{\|})$. The resulting eigenvalue equations are of the same form as in the parabolic case, but somewhat more complicated. The anisotropy of the bulk conduction band is included, and it is found to have a larger effect in quantum wells than in the bulk. The results can be expressed in terms of the perpendicular mass, which is relevant for the determination of confinement energies, and the parallel mass, which gives the curvature of $E(\mathbf{k}_{\|})$ at the bottom of a subband. We derive approximate expressions for these masses in the form of explicit functions of the confinement energy, which is experimentally accessible. The enhancement of the parallel mass relative to the bulk mass is found to be 2–3 times stronger than that of the perpendicular mass. It is shown that the boundary conditions need to be modified in the nonparabolic case. The nonintuitive result is that the confinement energy for the ground state usually is increased relative to a similar calculation in the parabolic approximation. We include the effect of a perpendicular magnetic field and derive an analytic expression for the Landau levels. The cyclotron mass is found to increase with magnetic field and approach the parallel mass in the limit of small magnetic fields. The parallel mass is also relevant for transport parallel to the layers, density of states, and exciton properties. The agreement with experiment is encouraging. Previous theoretical approaches are critically reviewed and the differences and similarities with this work are pointed out.

I. INTRODUCTION

The energy levels in narrow semiconductor quantum wells are of considerable interest both experimentally and theoretically. In this case the electron levels are of the order 100 meV above the bulk conduction-band edge, and it is expected that corrections due to conduction-band nonparabolicity can be important. Most of the work so far has been related to the shift of the confinement energy. Many theoretical approaches have been presented and have given partly conflicting results. The relations between these approaches and the reasons for the discrepancies have not been analyzed in detail previously. Another interesting problem which has received less attention is the modification of the energy dispersion parallel to the layers. The curvature at the bottom of a subband does not necessarily correspond to the same effective mass as in the bulk. Furthermore one can expect the subband dispersion to deviate from parabolicity. The three effects of nonparabolicity on the subband structure of a quantum well are shown schematically in Fig. 1.

Most calculations of semiconductor heterostructures have applied the envelope-function method. A common way to include nonparabolicity effects in this scheme is to include a small number of bands in a matrix equation and preferably treat the other bands in perturbation theory. The latter has the effect of modifying the effective masses. Such matrices were derived by Kane[1] for the bulk case and adapted to the superlattice case by Bastard whose original model[2] included the (lowest) conduction band, the light-hole band, and the heavy-hole band, which is decoupled from the other bands when $\mathbf{k}_{\|}$, the wave vector parallel to the interfaces, is zero. This model has later been extended to include the split-off band.[3] Similar equations have been presented by Yamada *et al.*[4] Implicit equations for the energy are given which are easy to solve numerically. Rössler[5] has, however, pointed out that one also needs to include higher conduction bands (of symmetry $\Gamma_8+\Gamma_7$) for an accurate description of the

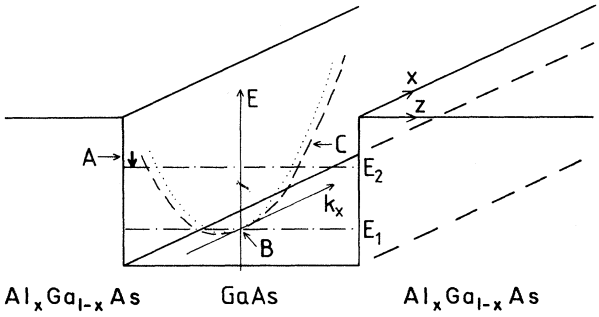

FIG. 1. Schematic picture of the effects of nonparabolicity in a quantum well. (*A*) The confinement energies are shifted. (*B*) The curvature at the bottom of a subband corresponds to a parallel mass, which is different from the bulk mass. (*C*) The subband dispersion (dashed line) deviates from parabolicity (dotted line).

conduction band more than 50 meV above the band edge. Much of the anisotropy of the lowest conduction band comes from the interaction with these bands. In this way one ends up with a 14×14 matrix, whose eigenvalues give the energy dispersions in the bulk. The use of such a matrix together with proper boundary conditions for a quantum well or the roughly triangular potential at a modulation-doped semiconductor interface would be very cumbersome. A more convenient method is to obtain the bulk dispersion from this matrix once and for all and from this determine the coefficients in an expansion of the energy dispersion up to fourth order in k. Such a method has been used for the two-dimensional electron gas at the $GaAs/Al_xGa_{1-x}As$ interface by Malcher *et al.*[6] The problem was first solved self-consistently in the parabolic approximation, and then the higher-order terms were included in perturbation theory. A similar approach with a position-dependent effective mass was proposed by Lassnig.[7] This position dependence arises because the conduction-band edge is at a different energy separation from a sublevel at different distances from the interface. In the approaches of Refs. 6 and 7 it is also straightforward to include the spin splitting and the effect of a magnetic field perpendicular to the interfaces.

In this paper we point out that for a square well the nonparabolic subband structure can be determined essentially analytically. A short version of this work was presented recently.[8] The energies are obtained from implicit equations of the same form as in the parabolic case. This approach also gives particular insight into the relation between the suitably defined perpendicular mass, which determines the shift of the confinement energies, and the parallel mass, which gives the curvature at the bottom of a subband. Recently[9] we pointed out the important difference between these two masses using simplified boundary conditions. In this article we make a more thorough analysis and demonstrate that the conclusions in Ref. 9 remain qualitatively correct but change slightly quantitatively. We start from an accurate expression for the bulk conduction-band dispersion expanded up to fourth order in k. The anisotropy of the bulk conduction band is included. The method can in principle be applied to any pair of direct-band-gap semiconductors but is here applied to GaAs quantum wells surrounded by $Al_{0.3}Ga_{0.7}As$. The results are particularly clearly brought out in the case of infinite barriers, as shown in Sec. II. The more realistic case with finite barriers is treated in Sec. III. In this case a more careful analysis of the boundary condition is required. The details are found in the Appendix. In Sec. IV we derive an expression for the Landau levels in a perpendicular magnetic field and calculate the cyclotron mass, which can be measured experimentally. We compare our results with some recent experiments and other theories in Sec. V and the conclusions follow in Sec. VI.

II. INFINITE QUANTUM WELL

The conduction-band dispersion in the bulk of a direct-band-gap III-V compound semiconductor expanded up to fourth order in k is of the form

$$E(\mathbf{k})=\frac{\hbar^2k^2}{2m}+\alpha_0k^4+\beta_0(k_x^2k_y^2+k_y^2k_z^2+k_z^2k_x^2) \pm\gamma_0[k^2(k_x^2k_y^2+k_y^2k_z^2+k_z^2k_x^2) -9k_x^2k_y^2k_z^2]^{1/2} . \quad (1)$$

Here m is the effective mass in the relevant material. The parameters α_0, β_0, and γ_0 are all negative and have been determined from a 14-band $\mathbf{k}\cdot\mathbf{p}$ calculation, which has been described in detail by Braun and Rössler.[10] The values of GaAs and $Al_{0.3}Ga_{0.7}As$ were given in Ref. 6 and are reproduced in Table I. For other materials the values can be determined from explicit expressions given

TABLE I. Parameters used in this calculation (including the models in Refs. 3 and 12).

	GaAs	$Al_{0.3}Ga_{0.7}As$
Electron mass	0.0665	0.095
Nonparabolicity parameters		
α_0 (eV Å^4)	−2107	−1164
α' (eV^{-1})	0.642	0.724
β_0 (eV Å^4)	−2288	−1585
β' (eV^{-1})	0.697	0.985
γ_0 (eV Å^3)	−27.57	−22.74
Valence-band parameters		
γ_1^L	6.85	5.83
γ_2^L	2.1	1.674
Kane matrix element P (a.u.)	0.6778	0.6778
Energy gap (meV)	1519	1921
Spin-orbit splitting (meV)	341	321
Conduction-band discontinuity (meV)	261	
Valence-band discontinuity (meV)	141	

in Ref. 10. The last term describes the spin splitting which is due to the lack of inversion symmetry in GaAs. In the present article we have not included the spin splitting exactly but it can be included as a perturbation, as discussed in Sec. III. We keep the anisotropic fourth-order term (proportional to β_0) which often has been neglected by previous authors. The layered structure is assumed to be grown along the [001] direction. If we collect the k_z terms separately we can rewrite the first three terms

$$E(\mathbf{k})=\alpha_0 k_z^4+\left[\frac{\hbar^2}{2m}+(2\alpha_0+\beta_0)(k_x^2+k_y^2)\right]k_z^2 + \frac{\hbar^2}{2m}(k_x^2+k_y^2)+(2\alpha_0+\beta_0)k_x^2k_y^2 + \alpha_0(k_x^4+k_y^4) . \quad (2)$$

We follow the prescription of effective-mass theory[11] and use this expression for the kinetic energy with the replacement $k_z \rightarrow -i\,d/dz$. The potential $V(z)$ of the quantum well, which extends from $z=-b$ to $z=b$, is then added. We still have translational invariance parallel to the layers of the quantum well, and therefore k_x and k_y remain good quantum numbers.

We first consider the confinement energies in a quantum well with infinite barriers and put k_x and k_y equal to zero. It is immediately verified that the solutions of the Schrödinger equation are of the form $\cos Kz$ and $\sin Kz$ for states with even and odd parity, respectively, just like in the parabolic case. The boundary conditions (vanishing wave function at the interfaces) are still fulfilled if

$$K=\frac{n\pi}{2b}, \quad n=1,2,\ldots . \quad (3)$$

Odd n applies to even parity solutions and vice versa. The only difference compared to the parabolic case is that the relation between the energy and the parameter K is altered. We have

$$\varepsilon=\alpha_0 K^4+\frac{\hbar^2K^2}{2m} . \quad (4)$$

We have here introduced ε for the confinement energy: $\varepsilon \equiv E(k_\parallel=0)$, where $k_\parallel=(k_x^2+k_y^2)^{1/2}$. If we invert expression (4) we obtain

$$K=\left[\frac{m}{\alpha'\hbar^2}[1-(1-4\alpha'\varepsilon)^{1/2}]\right]^{1/2} , \quad (5)$$

where

$$\alpha' \equiv -\left[\frac{2m}{\hbar^2}\right]^2\alpha_0 . \quad (6)$$

For GaAs $\alpha'=0.64\ \mathrm{eV}^{-1}$. We are usually interested in energies for which $\alpha'\varepsilon \ll 1$ and after expanding the inner square root we obtain

$$K\approx\frac{[2m\varepsilon(1+\alpha'\varepsilon)]^{1/2}}{\hbar} . \quad (7)$$

In the parabolic case we would just have $K=(2m\varepsilon)^{1/2}/\hbar$. The term $(1+\alpha'\varepsilon)$ thus represents the nonparabolicity correction to the lowest order. It is often convenient to express nonparabolicity effects in terms of an energy-dependent effective mass and the natural choice in the present case is

$$m_\perp(\varepsilon)\approx m(1+\alpha'\varepsilon) . \quad (8)$$

We call this the perpendicular mass. A more accurate definition follows from Eq. (5):

$$m_\perp(\varepsilon)=\frac{m}{2\alpha'\varepsilon}[1-(1-4\alpha'\varepsilon)^{1/2}] . \quad (9)$$

It should be noted that $m_\perp$ is only intended for the calculations of confinement energies. For example, it is not related to transport properties or energy dispersion along the z direction in a superlattice.

We next consider the parallel dispersion and let k_x and k_y be different from zero. It is clear that the energy dispersion for the quantum well is given by Eq. (2) with k_z replaced by $K=n\pi/2b$. The coefficient of the $k_\parallel^2$ term becomes

$$\frac{\hbar^2}{2m}+(2\alpha_0+\beta_0)K^2 . \quad (10)$$

It is appropriate to define the energy-dependent parallel mass $m_\parallel(\varepsilon)$ by equating this coefficient to $\hbar^2/[2m_\parallel(\varepsilon)]$. In similarity to Eq. (6) we define the constant

$$\beta' \equiv -\left[\frac{2m}{\hbar^2}\right]^2\beta_0 , \quad (11)$$

where $\beta'=0.70\ \mathrm{eV}^{-1}$ for GaAs. To lowest order in ε we then find

$$m_\parallel(\varepsilon)\approx m[1+(2\alpha'+\beta')\varepsilon] . \quad (12)$$

Comparison with $m_\perp(\varepsilon)$, Eq. (8), shows that *the parallel mass is enhanced over the bulk mass about three times more than the perpendicular mass.* We will find that this remains approximately true for finite wells, which are not too narrow. The expressions (8), (9), and (12) also hold for excited states, and in the present approximation the effective masses are only functions of the confinement energy.

It is worth noting that the anisotropy term has a larger influence in a quantum well than in the bulk. It is found from Eq. (1) that the k^4 term is proportional to α_0 in the [100] direction and $\alpha_0+\beta_0/3$ in the [111] direction in the bulk (the spin-splitting vanishes in these directions). In the quantum-well case the coefficient of β_0 is half of that of α_0 in the expression for $m_\parallel$.

III. FINITE QUANTUM WELL

The simple decoupling between the motion perpendicular and parallel to the layers is not possible anymore in the more realistic case with finite barriers, but it is possible to derive eigenvalue equations for the subband structure, which are not much more complicated in the non-

parabolic case than in the parabolic case. We consider a quantum well of GaAs of width $2b$ surrounded by $Al_{0.3}Ga_{0.7}As$ barriers of height V. The effective mass and nonparabolicity parameters in the well are denoted by m_1, α_{01}, and β_{01}, respectively, and the corresponding parameters in $Al_xGa_{1-x}As$ are m_2, α_{02}, and β_{02}. They are taken from Ref. 6 and given in Table I.

We first consider the case $k_x=k_y=0$. As an *Ansatz* we write down solutions of the same form as in the parabolic case:

$$F(z)=\begin{cases} B\cos(Kz), & |z|<b \quad (13a)\\ C\exp(-\lambda|z|), & |z|>b \quad (13b)\end{cases}$$

for even parity and

$$F(z)=\begin{cases} B\sin(Kz), & |z|<b \quad (14a)\\ C\exp(-\lambda z), & z>b \quad (14b)\\ -C\exp(\lambda z), & z<-b \quad (14c)\end{cases}$$

for odd parity. Here B and C are normalization constants. It is readily verified that the solutions in the nonparabolic case are still of the same form. One difference compared to the parabolic case is that the relation between the parameters K and λ and the energy is more complicated. K is still given by Eq. (5) (with m and α' replaced by m_1 and α_1') and

$$\lambda=\left[\frac{m_2}{\alpha_2'\hbar^2}\{[1+4\alpha_2'(V-\varepsilon)]^{1/2}-1\}\right]^{1/2}. \quad (15)$$

This relation can be used to define a perpendicular mass in the barrier. This is actually derived from the energy dispersion above the conduction-band edge in the barrier material, and it is uncertain how far into the band gap one can extrapolate that expression. It would be appropriate to take the decay constant in the energy gap from a calculation of the complex band structure,[12,13] in which the wave vector is imaginary in the band gap. However, since the subband structure is fairly insensitive to the effective mass in the barrier for the well widths considered here,[12] we prefer to use the analytical expression (15). It is not difficult to insert the expressions for K and λ in the eigenvalue equation to be derived below and search for the energies satisfying this equation.

In the nonparabolic case we must also pay some attention to the boundary conditions. In a previous paper[9] we simply used the common boundary conditions[2,14] with continuity of the envelope function F and its derivative divided by the bulk mass. A proper determination of the boundary conditions should actually impose continuity of the total wave function and its derivative and one should calculate both the envelope functions and the Bloch functions $u(z)$ which have the periodicity of the lattice. Such boundary conditions have been derived by Burt.[15] Calculations explicitly including $u(z)$ have been performed by Smith and Mailhiot.[13] They are rather laborious and beyond the scope of this article. We instead consider reasonable boundary conditions for the envelope function and analyze how consistent results they give. A common way of deriving boundary conditions is to integrate the Schrödinger equation from $-\delta$ to δ (if the boundary is at $z=0$) and let $\delta\to 0$. Since the effective masses and the nonparabolicity parameters are position dependent the Hamiltonian should first be written in Hermitian form. This can be done in the following way:

$$H=-\frac{d}{dz}\frac{\hbar^2}{2m}\frac{d}{dz}+\frac{d^2}{dz^2}\alpha_0\frac{d^2}{dz^2}+V(z)\,. \quad (16)$$

Integration from $-\delta$ to δ then gives continuity of

$$\frac{\hbar^2}{2m}\frac{dF}{dz}-\alpha_0\frac{d^3F}{dz^3}-\frac{d\alpha_0}{dz}\frac{d^2F}{dz^2}\,. \quad (17)$$

If we ignore the difference between α_0 in the well and in the barriers we obtain the results derived by de Dios Leyva *et al.*[16] These boundary conditions are very convenient because it turns out that they give exactly the same result as if one imposes continuity of the envelope function and its derivative divided by the energy-dependent perpendicular mass given by Eq. (9).

However, the derivation of these boundary conditions is not quite indisputable. One has to let δ go to zero to make the potential-energy terms vanish. But the derivative of the envelope function is discontinuous at the interface, if we take it to be a step function, and then the third derivative is singular at the interface. Furthermore we should take into account that α_0 is different in the two materials. In the Appendix we derive the current density for a potential step in the nonparabolic case. It is found that the current density is conserved if the boundary conditions described above are modified to include a factor 2 in the third-order term of (17). Consideration of the current density has the advantage that it should be the same for all values of z including those some distance from the interface. In practice the potential at the interface drops rapidly but continuously over a few atomic layers. This makes the expression for the current density mathematically well-behaved but complicated in the interface region. However, away from this region we can easily evaluate the current density in the bulk regions.

After applying the three considered boundary conditions the eigenvalue equations can be summarized in the equation

$$\tan(Kb)=\frac{\frac{\hbar^2\lambda}{2m_2}-N\alpha_{02}\lambda^3}{\frac{\hbar^2K}{2m_1}+N\alpha_{01}K^3} \quad (18)$$

for even-parity states with $\tan Kb$ replaced by $-\cot Kb$ for odd-parity states. Here N is an integer which depends on the boundary conditions chosen. $N=0$ corresponds to the same boundary conditions as in the parabolic case. Integration of the Schrödinger equation from $-\delta$ to δ

and neglecting the discontinuity of α_0 and dF/dz corresponds to $N=1$. This boundary condition is equivalent to continuity of F and $m_\perp(\varepsilon)^{-1}dF/dz$. Finally $N=2$ represents the modification necessary to make the boundary conditions compatible with current conservation. The analysis in the Appendix does not imply that the boundary conditions given by $N=2$ are the correct ones, which should involve the cell-periodic functions $u(z)$. The mathematical difficulties described above occur both for $N=1$ and $N=2$. What we want to point out is that for $N=2$ (but not for $N=1$) we obtain relations between the amplitudes of the incoming, reflected, and transmitted waves at a potential step which are consistent with current density conservation. We have verified that for very high barriers all three boundary conditions lead to a decrease of the confinement energy in the nonparabolic case relative to the parabolic case in agreement with Eq. (4). (Note that α_0 is negative.)

In Fig. 2 we show the confinement energy for the ground state as a function of well width in different approximations. The simplest boundary conditions, $N=0$, always imply a reduction of the confinement energy relative to the parabolic case. This is also what one might expect intuitively: The effective mass increases as we go higher up in the conduction band and a higher mass leads to a lowering of the energy levels. But since the boundary conditions also depend on the effective masses it turns out that a more careful consideration of them can lead to an increase of the confinement energy. For $N=1$ this increase is rather small but for $N=2$ it can be substantial. It would be interesting if one could compare the results of these fairly simple boundary conditions to the exact expressions derived by Burt[15] together with an explicit calculation of the cell-periodic part of the total wave function. It should be noted that for excited states the energy is usually lowered by the nonparabolicity effects for all boundary conditions and when this lowering is substantial, the difference between the boundary conditions has a rather small effect. In Table II we give the confinement energies for the lowest state in a 50- and a 100-Å quantum well for different boundary conditions together with the results of some other models described below.

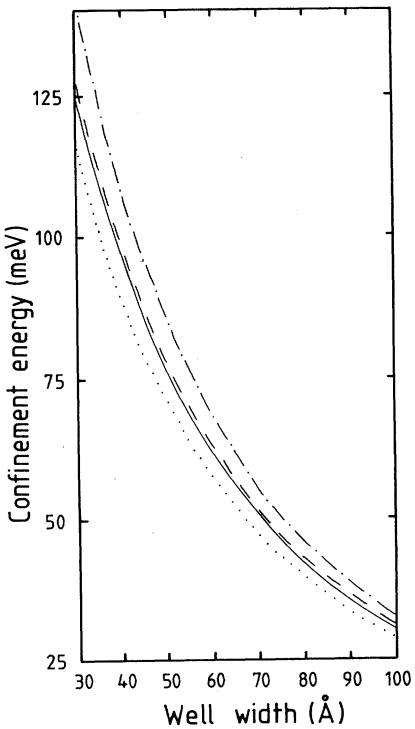

FIG. 2. Well-width dependence of the confinement energy for the ground state in a GaAs quantum well surrounded by $Al_{0.3}Ga_{0.7}As$ in different approximations. The solid line shows the parabolic approximation and the other lines the nonparabolic case with different boundary conditions characterized by the integer N in Eq. (18). The dotted line ($N=0$) corresponds to the same boundary conditions as in the parabolic case. The dashed line ($N=1$) corresponds to continuity of the envelope function and its derivative divided by the perpendicular mass (9). The dashed-dotted line ($N=2$) represents the modification necessary for conservation of the current density.

We next consider the modifications that need to be made when the wave vector parallel to the layers $\mathbf{k}_\parallel$ is different from zero. In the Appendix the constant A is defined as the coefficient of the k_z^2 term. This term is now given by

$$A=\frac{\hbar^2}{2m}+(2\alpha_0+\beta_0)k_\parallel^2 . \tag{19}$$

The boundary conditions thus explicitly depend on the parallel wave vector. Another modification is that the energy E now depends on the parameter K and the quantum numbers k_x and k_y. This relation is found by letting the Hamiltonian (2) operate on the envelope functions (13) and (14). We next have to invert this expression and express K in terms of E, k_x, and k_y. The result is

$$K=\left\{G_1\left[1-\left[1-\frac{G_2}{G_1^2}\right]^{1/2}\right]\right\}^{1/2} , \tag{20}$$

where

$$G_1=\frac{m_1}{\alpha_1'\hbar^2}-\frac{2\alpha_1'+\beta_1'}{2\alpha_1'}k_\parallel^2 \tag{21a}$$

and

$$G_2=\frac{4m_1^2E}{\alpha_1'\hbar^4}-\frac{2m_1}{\alpha_1'\hbar^2}k_\parallel^2+k_\parallel^4+\frac{\beta_1'}{\alpha_1'}k_x^2k_y^2 . \tag{21b}$$

For λ we similarly obtain

$$\lambda=\left\{G_3\left[\left[1+\frac{G_4}{G_3^2}\right]^{1/2}-1\right]\right\}^{1/2} , \tag{22}$$

where

$$G_3=\frac{m_2}{\alpha_2'\hbar^2}-\frac{2\alpha_2'+\beta_2'}{2\alpha_2'}k_\parallel^2 \tag{23a}$$

and

$$G_4=\frac{4m_2^2(V-E)}{\alpha_2'\hbar^4}+\frac{2m_2}{\alpha_2'\hbar^2}k_\parallel^2-k_\parallel^4-\frac{\beta_2'}{\alpha_2'}k_x^2k_y^2 . \tag{23b}$$

For different values of k_x and k_y one can find the values of E satisfying the eigenvalue equation (18). In this way one can determine the parallel dispersion of the subbands. This will be referred to as the "exact" solution. It is not much more difficult to write a short computer program for this case than for the parabolic case. However, it does not give much physical insight into the relation between the perpendicular and the parallel mass.

We have, therefore, derived simple approximations which give the parallel mass as an explicit function of the confinement energy. First the eigenvalue problem for $k_{\parallel}=0$ is solved as described above. Then the terms including $k_{\parallel}$ are treated in first-order perturbation theory. This procedure should be appropriate for the small $k_{\parallel}$ values considered here. We are particularly interested in the coefficient of the $k_{\parallel}^2$ term, and we thus want to calculate the expectation value of

$$\frac{\hbar^2}{2m}-\frac{d}{dz}(2\alpha_0+\beta_0)\frac{d}{dz} . \tag{24}$$

For the first term the result is simply

$$\frac{\hbar^2}{2m_1}P_w+\frac{\hbar^2}{2m_2}P_b , \tag{25}$$

where P_w (P_b) is the probability that the electron is in the well (barrier) given by

$$P_w=B^2\left[b\pm\frac{\sin(2Kb)}{2K}\right] \tag{26a}$$

and

$$P_b=B^2\frac{1\pm\cos(2Kb)}{2\lambda} . \tag{26b}$$

Here the upper (lower) sign applies to states with even (odd) parity. B is the normalization constant in Eqs. (13) and (14) given by

$$B=\left[b\pm\frac{\sin(2Kb)}{2K}+\frac{1\pm\cos(2Kb)}{2\lambda}\right]^{-1/2} . \tag{27}$$

Equation (25) describes the enhancement of the effective mass which occurs even in the absence of nonparabolicity terms and which is due to the penetration of the wave function into the barriers, where the effective mass is larger. It is clear that in the limit of zero well width the parallel mass should be that of the barrier material. This effective mass has been calculated exactly by Priester *et al.*[17] and a comparison with their expression shows that Eq. (25), which is derived with the use of perturbation theory, is in fact an exact result. It is interesting that the same expression recently has been obtained in a different context: Johnson and MacKinnon[18] have shown that in the parabolic approximation the effective electron mass for motion along the magnetic field parallel to a heterojunction is also given by Eq. (25).

Caution is necessary to evaluate the second term in Eq. (24). The discontinuities of the parameters α_0 and β_0 and the derivative of the envelope function at the interfaces must be taken into account. The matrix element turns out to be

$$B^2\left[(2\alpha_{01}+\beta_{01})K\left[bK\mp\frac{\sin(2kb)}{2}\right]+(2\alpha_{02}+\beta_{02})\lambda\frac{1\pm\cos(2Kb)}{2}\right] \tag{28}$$

for even (odd) parity as before. Adding this to expression (25) we obtain an explicit expression of the parallel mass as a function of ε,

$$m_{\parallel}(\varepsilon)=B^{-2}\left[\left[1-(2\alpha_1'+\beta_1')\frac{\hbar^2K^2}{2m_1}\right]\frac{b}{m_1}\pm\left[1+(2\alpha_1'+\beta_1')\frac{\hbar^2K^2}{2m_1}\right]\frac{\sin(2Kb)}{2m_1K}+\left[1-(2\alpha_2'+\beta_2')\frac{\hbar^2\lambda^2}{2m_2}\right]\times\frac{1\pm\cos(2Kb)}{2m_2\lambda}\right]^{-1} . \tag{29}$$

Applying some approximations we can simplify it further. If the penetration of the wave function into the barriers is small the term proportional to b dominates the expressions (27) and (28). We can then also neglect the mass enhancement described in (25). If we further expand K to lowest order in ε we recover (12), which was derived under the assumption of infinite barriers. Taking the barriers to be finite decreases both the perpendicular and parallel mass since ε decreases, but the expressions (8) and (12) remain approximately true. In Fig. 3 we give the parallel dispersion for the ground state in a 50-Å GaAs quantum well between $Al_{0.3}Ga_{0.7}As$ barriers for different cases: the exact solution of Eqs. (18)–(23) for $N=0$, 1, and 2, using the simple approximation (12) for the parallel mass for $N=2$ and ignoring nonparabolicity

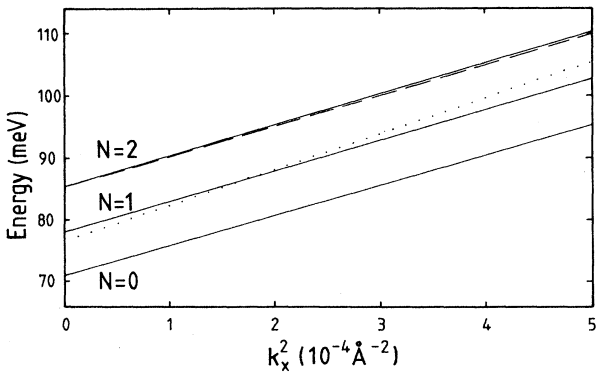

FIG. 3. Energy vs the square of k_x for the ground subband in a 50-Å GaAs quantum well. The dotted line shows the parabolic approximation and the solid lines the exact solution of Eq. (18) modified by Eq. (19) for $N=0$, 1, and 2. For $N=2$ the dispersion with the simple approximation (12) for the parallel mass is also shown (dashed line). The slope is inversely proportional to the parallel mass. The solid lines deviate from straight lines slightly.

effects. It is seen that the parallel dispersion in the nonparabolic case is not much influenced by the boundary conditions and that the parallel mass is clearly lower in the parabolic case. (The slope is steeper.) It is also found that the simple approximation (12) is quite good even for such a narrow well as 50 Å. In Fig. 4 we give the perpendicular and the parallel masses defined by Eqs. (9) and (29), respectively, as a function of well width. As the well width decreases the confinement energy and thereby both the masses increase. It is seen that the parallel mass is clearly higher than the perpendicular mass for all well widths. For a 100-Å well the enhancement of the parallel mass is about three times stronger, in agreement with the simple expressions (8) and (12). For narrower wells this factor decreases, but even for the thinnest well considered, 30 Å, the enhancement of $m_{\parallel}$ is twice that of $m_{\perp}$.

One can estimate the spin-splitting following Malcher *et al.*[6] The kinetic energy can be described by a 2×2 matrix whose eigenvalues are given by (1). In principle there can be a contribution to the spin-splitting from the inversion asymmetry in bulk GaAs and from a built-in electric field. The latter gives a contribution for the single interface case considered in Ref. 6 but it vanishes for a symmetric quantum well. Using the parabolic case as the zeroth-order Hamiltonian, Malcher *et al.* derive an expression for the spin splitting, whose dominating term for small $\mathbf{k}_{\parallel}$ is

$$\left\langle \frac{d}{dz}\gamma_0\frac{d}{dz}\right\rangle k_{\parallel} \tag{30}$$

in the present notation. The explicit expression in the quantum-well case for this matrix element is given by Eq. (28) with $(2\alpha_0+\beta_0)$ replaced by γ_0.

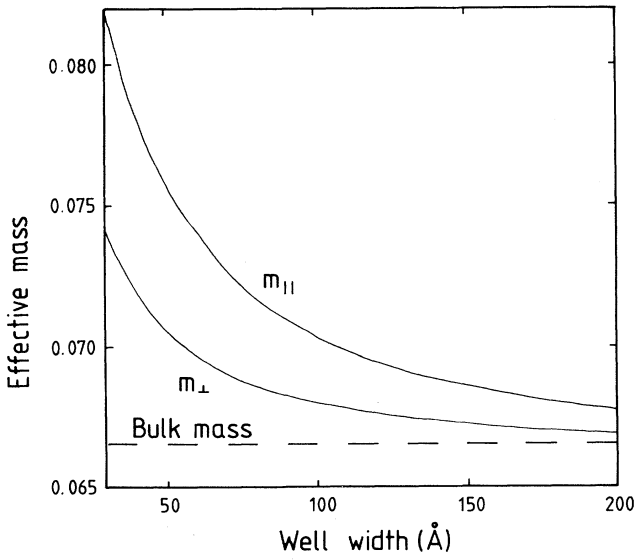

FIG. 4. Well-width dependence of the parallel mass according to Eq. (29) and the perpendicular mass [Eq. (9)] in units of the free-electron mass.

IV. EFFECT OF MAGNETIC FIELD

In the present formalism it is straightforward to include the effect of a magnetic field perpendicular to the interfaces and in this way directly compare with results of cyclotron resonance experiments. As before we take the solution for $\mathbf{k}_{\parallel}=0$ as the zeroth-order Hamiltonian and include the terms involving $\mathbf{k}_{\parallel}$ in perturbation theory. The magnetic field quantizes the motion in the x-y plane and the continuous variables k_x and k_y are replaced by the Landau level index n. The procedure for inclusion of a magnetic field is to replace $\mathbf{k}$ by $\mathbf{k}+e\,\mathbf{A}/\hbar$, where $\mathbf{A}$ is the vector potential. With a magnetic field in the z direction, k_x and k_y do not commute:

$$[k_x, k_y]=-\frac{ieB}{\hbar}\ . \tag{31}$$

Therefore we must replace $k_x k_y$ by the anticommutator $\{k_x\, k_y\}$. We follow the standard procedure to introduce harmonic oscillator operators $a^{\dagger}$ and a defined by

$$a^{\dagger}=\left[\frac{\hbar}{2eB}\right]^{1/2}(k_x+ik_y) \tag{32a}$$

and

$$a=\left[\frac{\hbar}{2eB}\right]^{1/2}(k_x-ik_y)\ . \tag{32b}$$

They have the well-known properties

$$au_n=\sqrt{n}\,u_{n-1} \tag{33a}$$

and

$$a^{\dagger}u_n=\sqrt{n+1}\,u_{n+1}\ . \tag{33b}$$

Here u_n is a harmonic oscillator function with the Landau level index $n=0,1,2,\ldots$. When the operators in expression (2) operate on u_n they give terms proportional to u_n with the exception of $(a^{\dagger})^4$ and a^4 which give terms proportional to u_{n+4} and u_{n-4}, respectively. These terms can be treated in second-order perturbation theory. (The first-order correction vanishes.) If we use the parabolic terms as the zeroth-order Hamiltonian, we find that this correction is

$$\frac{\beta_0^2 m_{\parallel} e^3 B^3}{8\hbar^5}(2n^3+3n^2+7n+3)\ . \tag{34}$$

Here the prefactor $\beta_0^2 m_{\parallel} e^3/\hbar^5$ is of the order 10^{-7} meV T^{-3}, so we can safely neglect the terms involving $(a^{\dagger})^4$ and a^4. When we let the other operators in (2) operate on u_n we find

$$E_n(B)=\varepsilon+\left\langle\frac{\hbar^2}{2m}-\frac{d}{dz}(2\alpha_0+\beta_0)\frac{d}{dz}\right\rangle\frac{2eB}{\hbar}(n+\tfrac{1}{2})$$
$$+[(8n^2+8n+5)\langle\alpha_0\rangle$$
$$+(n^2+n+1)\langle\beta_0\rangle]\frac{e^2B^2}{2\hbar^2}\ . \tag{35}$$

The expectation value in the second term is just $\hbar^2/(2m_{\parallel})$ according to the definition (24). If the layer

width is not too small we can also replace the expectation values of the nonparabolicity parameters by the values in the well. Reintroducing α_1' and β_1' we then obtain

$$E_n(B)=\varepsilon+(n+\tfrac{1}{2})\frac{\hbar eB}{m_\parallel} -\tfrac{1}{8}[(8n^2+8n+5)\alpha_1' +(n^2+n+1)\beta_1']\left[\frac{\hbar eB}{m_1}\right]^2 . \quad (36)$$

For small magnetic fields the last term can be neglected and we can write

$$E_n(B)\approx\varepsilon+(n+\tfrac{1}{2})\frac{\hbar eB}{m_\parallel} . \quad (37)$$

The cyclotron mass is defined by the relation

$$m_c=\frac{\hbar eB}{\Delta E(B)} , \quad (38)$$

where $\Delta E(B)$ is the energy difference between two Landau levels, which is what is measured in cyclotron-resonance experiments. From (37) and (38) we can easily verify that *in the limit $B\rightarrow 0$ the cyclotron mass is equal to the parallel mass.*

If we consider the difference $\Delta E_n(B)=E_{n+1}(B)-E_n(B)$ for magnetic fields high enough that the last term in (36) cannot be neglected, we find

$$\Delta E_n(B)=\frac{\hbar eB}{m_\parallel}-\tfrac{1}{4}(8\alpha_1'+\beta_1')(n+1)\left[\frac{\hbar eB}{m_1}\right]^2 . \quad (39)$$

Thus the cyclotron mass increases with B and the Landau level index n. We should, however, expect further corrections to the coefficient in front of B^2 due to confinement effects. The correction to $m_\parallel$ came from terms proportional to $k_z^2k_\parallel^2$ in the bulk expression (2). If it were expanded to sixth order, there would be terms proportional to $k_z^2k_\parallel^4$, which would give corrections to the coefficient in front of B^2 in Eq. (35). In the calculations by Malcher *et al.*[6] for a single interface these terms have been neglected and there should also be similar corrections to the Landau levels at finite magnetic fields.[19]

V. COMPARISON WITH EXPERIMENT AND OTHER THEORETICAL MODELS

There are many experimental results related to the confinement energies in quantum wells. Unfortunately there is a considerable spread[20] among the results for narrow quantum wells, where the nonparabolicity effects are the strongest. Possible explanations for this are uncertainty in the well width, grading of the interfaces, and influence of the minima at the X points in the Brillouin zone. Therefore we concentrate here on experiments which measure the parallel dispersion. Several such experiments have been performed for modulation-doped heterojunctions where the present theory is not immediately applicable, but fewer experiments have been performed for undoped quantum wells. Singleton *et al.*[21] have performed cyclotron-resonance experiments for a 22-Å GaAs quantum well between $Al_{0.36}Ga_{0.64}As$ barriers. The cyclotron mass was found to approach 0.083 in the limit of small magnetic fields. The present calculation yields a parallel mass of 0.080 in good agreement with experiment. The cyclotron mass was found to increase rapidly with magnetic field in qualitative agreement with the prediction in the previous section where it was mentioned that the present theory with the bulk dispersion expanded up to fourth order in k is insufficient for a quantitative comparison. The confinement energy for this sample was found to be 198 meV from photoconductivity experiments. This is clearly higher than the calculated energy in the parabolic approximation, 178 meV. Using boundary conditions with $N=2$ in Eq. (18) we have obtained a confinement energy of 205 meV. This agreement may be fortuitous because for such narrow wells the confinement energy is very sensitive to input parameters like well width and conduction-band discontinuity.

Cyclotron-resonance experiments for superlattices with 80-Å GaAs quantum wells and 20-Å $Al_xGa_{1-x}As$ barriers with x between 0.1 and 0.3 have been performed by Duffield *et al.*[22] With the magnetic field perpendicular to the layers they measured an effective mass slightly larger than 0.07, slowly increasing with x. For an isolated quantum well with the same parameters we obtain a parallel mass of 0.070 for $x=0.1$ and 0.072 for $x=0.3$. The remarkably good agreement is somewhat surprising because the overlap between the wave functions in adjacent quantum wells of the superlattice is considerable so the quantum wells can hardly be considered isolated. Duffield *et al.* also measured a much more enhanced mass with the magnetic field parallel to the layers when the electrons can tunnel through the thin barriers. This mass is sensitive to the width and height of the barriers and is not related to the perpendicular mass defined in this article for a single quantum well.

Interband magneto-optical experiments by Ancilotto *et al.*[23] with an 80-Å GaAs quantum well between $Al_{0.3}Ga_{0.7}As$ barriers could not be quantitatively explained by a six-band model with bulk parameters as input. The slope of the transition energy as a function of magnetic field, corresponding to the inverse parallel mass, could, however, be reproduced if the electron mass 0.074 were taken as input. This theory yields a parallel mass of 0.072. The comparison is not quite straightforward because the six-band model includes nonparabolicity effects to some extent. In total the agreement with experiment is encouraging although more experiments are desirable for a more certain evaluation of the theory.

Cyclotron-resonance experiments are often influenced by polaron effects,[24] which lead to an enhancement of the effective mass which is of the same order of magnitude as the effect of band nonparabolicity. So far these two effects have often been considered separately, which makes a straightforward comparison with experiment difficult. One of the virtues of the present approach is that it is simple enough that it could serve as the starting point of a calculation, which includes contributions to the effective mass both from band nonparabolicity and polaron effects. In the experiments mentioned above polaron effects were subtracted in Ref. 21 but not in Ref. 22.

We next turn to a comparison with other theoretical approaches. The use of energy-dependent effective masses has recently been subject to some controversy. An article by Welch, Wicks, and Eastman (WWE) (Ref. 25) was criticized by Hiroshima and Lang (HL),[26] who, in turn, were criticized by Nelson, Miller, and Kleinman (NMK).[27] Very recently Persson and Cohen (PC) (Ref. 28) questioned the use of energy-dependent effective masses in Ref. 27. These four articles only dealt with the confinement energies. The question whether one should use the concept of an energy-dependent effective mass is largely a matter of definition. HL call their method a solution of the Luttinger-Kohn equation in contrast to the energy-dependent effective-mass approach by WWE, but their method is in fact equivalent to the approach we used in our previous paper,[9] where we defined energy-dependent masses. The essential issues are rather how energy-dependent masses should be defined and how they should be used. The main difference between Refs. 25 and 26 lies in the definition of the effective mass. WWE take the effective mass to be the ratio between the momentum and the velocity, i.e.,

$$m(E)=\frac{p}{v}=\frac{\hbar^2 k}{\partial E/\partial k} . \tag{40}$$

With the dispersion (1) this gives a perpendicular mass $m_\perp = m(1+2\alpha'\varepsilon)$. As shown in the straightforward solution of the Schrödinger equation in Sec. II this is not the appropriate definition. HL invert the $E(k)$ expression which gives the correct relation $m_\perp = m(1+\alpha'\varepsilon)$.

The main difference between the approaches by Hiroshima and Lang[26] and by Nelson *et al.*[27] is how the energy-dependent effective mass is used. This is related to the boundary conditions. HL use the same boundary conditions as in the parabolic case, which corresponds to $N=0$ in Eq. (18), and also neglect the barrier nonparabolicity. NMK obviously use boundary conditions where the derivative of the envelope function is divided by the energy-dependent mass rather than the bulk mass, which corresponds to $N=1$ in Eq. (18). No clear argumentation is presented for this choice, which, however, is rather reasonable intuitively. The difference between our approach with $N=1$ and that of NMK lies partly in the choice of nonparabolicity parameters. We have taken our parameters from the bulk band structure calculated with a 14-band model[6] while NMK choose a nonparabolicity parameter $\gamma = 49$ Å^{-2} (Ref. 29), corresponding to $\alpha' = 0.86$ eV^{-1}, which is considerably more than the value derived in Ref. 6. NMK also estimate the nonparabolicity parameter in the barrier by assuming that γ is inversely proportional to the square of the band gap. This gives a value of α' which is much smaller than that given by Malcher *et al.*[6] The transcendental equation

$$\left[\frac{Km_2(E)}{\lambda m_1(E)}-\frac{\lambda m_1(E)}{Km_2(E)}\right]\tan(2Kb)=2 \tag{41}$$

from which NMK obtain their energies encompasses both the even-parity solutions and the odd-parity solutions in Eqs. (13) and (14). They find that the ground-state energies are increased somewhat but remain practically unchanged when nonparabolicity effects are included. Relative to our results with $N=1$ the confinement energies are influenced by the different input parameters, but the nonparabolicity shifts are similar. For the excited states we find that the levels are lowered much more when we use the expression (9) instead of the approximate expression (8), which is used by NMK. The difference between these expressions becomes particularly large for the 5-Å quantum well considered by NMK. It is seen that expression (9) is invalid when $\alpha'\varepsilon > \frac{1}{4}$. The reason for this is seen if the expression (4) is examined. The energy first increases with K but eventually it decreases again when the K^4 term starts to dominate. The maximum energy is $(4\alpha')^{-1}$. It is clear that higher-order terms are essential when this limit is approached. For GaAs the present theory becomes invalid for $\varepsilon > 0.4$ eV, and it can be expected to be dubious when $\varepsilon \approx 0.26$ eV, which is the case for a 5-Å quantum well. Furthermore, the effective-mass approximation cannot be expected to be valid for such narrow quantum wells.

Persson and Cohen[28] start from an expression including k^4 terms just like we did in our previous paper.[9] The boundary conditions are derived as in Ref. 16. The resulting eigenvalue equation is equivalent to that in NMK, as we have pointed out above. In contrast to the other papers PC find rather small energy shifts even for the excited states. They consider two nonparabolicity parameters which in the present notation correspond to $\alpha' = 0.123$ eV^{-1} and $\alpha' = 0.114$ eV^{-1} (Ref. 30). These values are thus only about one-fifth of the value calculated in Ref. 6, which is used in the present article. In similarity with the discussion in the previous paragraph, PC point out that the fourth-order expression (4) reaches a maximum before the dispersion bends down for large k. This expression has some similarity with the actual band structure for GaAs where the highest point of the conduction-band edge is about 2 eV above the Γ point. PC identify this point with the maximum of the fourth-order expression (4) and use this to determine the nonparabolicity parameter. This approach implicitly involves the dubious assumption that the fourth-order expression is valid up to the $\mathbf{k}$ value for which the conduction-band edge has a maximum, which according to the calculation by Chelikowsky and Cohen[31] is reached roughly one-third along the distance from the Γ point to the Brillouin zone boundary. It is found, however, that this point occurs at another k value in the actual band structure[31] than what Eq. (4) in Ref. 28 gives.

A commonly used expression for an energy-dependent electron mass was derived by Kolbas:[32]

$$m(E)=0.0665+0.0436E+0.236E^2-0.147E^3 . \tag{42}$$

This is actually an optical bulk mass[1,33] evaluated at 77 K. To lowest order it corresponds to $\alpha' = 0.656$ eV^{-1} and is fairly close to the perpendicular mass used in this article.

One of the first models which included nonparabolicity effects for quantum wells and superlattices was the Bastard model,[2,3] which is commonly used. It gives explicit transcendental equations, which also can be generalized to the case $\mathbf{k}_\parallel \neq 0$. It is based upon the Kane model[1]

where a certain number of bands are included exactly but the other bands are ignored. In the two-band model,[2] which includes the conduction band and the light-hole band, the effective mass is proportional to the band gap. The three-band model[3] also includes the split-off band. (The heavy-hole band is decoupled from these bands for $\mathbf{k}_{\parallel}=\mathbf{0}$.) One advantage with the Bastard model is that the boundary conditions are derived from many-band equations for the envelope functions and their first derivatives, and one avoids the mathematical difficulties associated with the singularities of the higher derivatives at a sharp interface.

A consistent use of the Bastard model is complicated by the neglect of remote bands. If we apply it with the effective masses used in this article and take the value for the Kane matrix element P, which describes the coupling between the conduction band and the valence band, from Ref. 34 (see Table I), we find that the ground-state confinement energy is decreased in the two-band model but increased in the three-band model relative to the parabolic case, as seen in Table II. However, these parameters are not consistent with the model. A consistent approach is to take the GaAs mass from experiment and determine P from this mass, the band gap, and (in the three-band model) the spin-orbit splitting. P is taken to be the same in $Al_xGa_{1-x}As$ as in GaAs. Then the effective mass in $Al_xGa_{1-x}As$ is calculated from P and the appropriate energy gaps. Both in the two-band model and the three-band model this mass turns out to be clearly smaller than in Refs. 35 and 36. In this way we obtain a slight increase of the confinement energies due to nonparabolicity effects, similar to what we obtain from Eq. (18) with $N=1$ (Ref. 37). For the two-band Bastard model, equations have also been given for $\mathbf{k}_{\parallel}\neq 0$ (Ref. 38). The enhancement of the parallel mass is found be to about $\frac{2}{3}$ of the value according to Eq. (29). The difference is well explained by the anisotropy term proportional to β_0, which is absent in the Bastard model.

TABLE II. Shift in meV of ground-state confinement energy relative to the parabolic case in different approximations. In the parabolic case the confinement energies are 76.7 meV for $L_z=50$ Å and 30.8 meV for $L_z=100$ Å.

L_z	50 Å	100 Å
This work, Eq. (18)		
$N=0$	−5.8	−1.5
$N=1$	+1.4	+0.6
$N=2$	+8.6	+2.5
Two-band Bastard model[a]		
$P=0.6778$ a.u.[b]	−9.8	−5.5
$P=0.7935$ a.u.[c]	+1.1	+0.5
Three-band Bastard model[d]		
$P=0.6778$ a.u.[b]	+5.5	+2.2
$P=0.6686$ a.u.[e]	+1.1	+0.5
Schuurmans and 't Hooft model[f]	+1.5	+0.7

[a]Reference 2.
[b]Effective masses and P value according to Table I.
[c]P chosen to reproduce m_1 in Table I. Shift relative to calculation in the parabolic case with $m_2=0.0841$ determined by this P value.
[d]Reference 3.
[e]P chosen to reproduce m_1 in Table I. Shift relative to calculation in the parabolic case with $m_2=0.0830$ determined by this P value.
[f]Reference 12. Parameters as in Table I.

The Bastard model has been further developed by Schuurmans and 't Hooft.[12] The conduction, heavy-hole, light-hole, and split-off bands are included in a matrix. This model also takes into account the modification of the effective masses due to remote bands (bands not included in the matrix). The numerical relation between E and k is obtained from a calculation of the band structure in the bulk materials. This involves the diagonalization of a 3×3 matrix (for $\mathbf{k}_{\parallel}=\mathbf{0}$). The secular equation can also be seen as a third-order equation in k^2 from which the desired $k(E)$ relation can be obtained analytically. The eigenvalue equations for the quantum-well case can be simplified for materials with relatively large band gaps into scalar equations for electrons and heavy holes and coupled equations for the light-hole and split-off bands. Boundary conditions with division of the envelope-function derivative by an energy-dependent mass corresponding to $N=1$ [Eq. (18)] are used. This model involves more numerical work than the previously mentioned approaches.

The application of this model in its original form involves some problems. Schuurmans and 't Hooft introduce four adjustable parameters, which in principle can be determined from the experimental values of m_e, m_{hh}, m_{lh}, and m_{so}, i.e., the effective masses for the conduction, heavy-hole, light-hole, and split-off bands, respectively. These four parameters include λ, which describes the coupling between the conduction band and the valence band and is proportional to P^2, and two modified Luttinger parameters γ_1 and γ_2, which are different from the "true" Luttinger parameters γ_1^L and γ_2^L (Ref. 39). The four inverse masses are expressed in Eqs. (9)–(12) in Ref. 12 in terms of these four parameters. By inverting these expressions it is found that λ becomes proportional to $m_{hh}^{-1}+m_{lh}^{-1}-2m_{so}^{-1}$. However, the sum of the first two terms is close to the third term. In fact, if the conduction band is not included in the matrix, the relations between these masses and the true Luttinger parameters are $m_{hh}=(\gamma_1^L-2\gamma_2^L)^{-1}$, $m_{lh}=(\gamma_1^L+2\gamma_2^L)^{-1}$, and $m_{so}=(\gamma_1^L)^{-1}$, and we obtain the result $\lambda=0$. The last of these relations is modified if the conduction band is included in the matrix as in Ref. 12 and a finite value of λ is obtained. Nevertheless, if experimental values of the hole masses are used, it is clear that λ becomes very sensitive to experimental uncertainties in the effective masses. In particular the mass of the split-off band is not known very accurately.

We have therefore modified the method by Schuurmans and 't Hooft so that we take the parameter P from Ref. 34 (Table I) and determine the other adjustable parameters s, γ_1, and γ_2 from the experimentally determined parameters m_e, γ_1^L and γ_2^L. It is seen in Table II

that for the ground state this gives a very good agreement with the present method if we use the same boundary conditions ($N=1$). For excited states the results often tend to fall in between those for $N=1$ and $N=2$. The method by Schuurmans and 't Hooft has recently been extended to the case of finite $\mathbf{k}_{\parallel}$ (Ref. 40). This involves much more numerical work and is outside the scope of the present article.

An alternative method to calculate the effective masses for a superlattice was recently given by Johnson *et al.*[41] They apply a sum rule for the oscillator strengths and determine both the parallel mass and a perpendicular mass, which is different from the one used in this paper. The enhancement of the parallel mass was about half of that determined experimentally by Duffield *et al.*[22] For the effective mass with the magnetic field parallel to the layers the agreement was about equally good as in the simpler Bastard model put forward in Ref. 22. In the latter case the dispersion along the superlattice direction is probed. In the limit of very wide barriers (corresponding to the isolated quantum wells considered in the present article) this dispersion becomes flat, i.e., the effective mass becomes infinite. For finite barriers the dispersion should not be expected to be parabolic over any substantial range of k values. It has been demonstrated[42] that this dispersion clearly deviates from a parabola also in the limit $k \rightarrow 0$.

VI. CONCLUSIONS

We have presented a convenient and fairly simple but quite accurate approach to determine the confinement energies in a quantum well and the effective masses for motion parallel to the interfaces. The subband structure can be obtained from transcendental equations of the same form as in the parabolic case but somewhat more complicated. The equations apply to excited states as well as the ground state. The approach should work well for semiconductors with band gaps large enough that the nonparabolicity can be properly described by a fourth-order expression in the relevant energy range. For small-band-gap semiconductors its usefulness is more limited, and it is not applicable to calculations of valence subband structures because of the strong coupling between heavy and light holes.

One of the main results is that the parallel mass is enhanced over the bulk mass 2–3 times more than the perpendicular mass. The modification of the boundary conditions due to nonparabolicity is analyzed. It is demonstrated that the confinement energy for the ground state can be *increased* when nonparabolicity effects are included, in agreement with the conclusion in Ref. 27 but in disagreement with most of the previous work. The parallel mass is not very sensitive to the boundary conditions. We explicitly include the effect of a magnetic field perpendicular to the interfaces and show that the parallel mass is equal to the cyclotron mass in the limit $B \rightarrow 0$. It is pointed out that sixth-order terms in k in the bulk expression are needed to calculate the increase of the cyclotron mass with B quantitatively. The parallel mass is also relevant for transport parallel to the layers (cf. the high electron-mobility transistor) and it has recently been used[43] in the calculation of exciton binding energies. The step in the density of states at the bottom of a subband is given by the parallel mass. Between the sublevels the density of states is not constant, as in the parabolic case, but increasing because of the nonparabolicity of the subband dispersion (effect C in Fig. 1). The agreement with recent experimental results is encouraging. We have also pointed out the differences and similarities with previous theoretical approaches, most of which have only been concerned with the shift of the confinement energies, and we have shed some light on the origin of the controversy between Refs. 25–28.

ACKNOWLEDGMENTS

During the course of this work I have benefitted from valuable discussions with many colleagues, in particular J. Singleton, R. J. Nicholas, J. D. White, E. P. O'Reilly, G. Fasol, M. Altarelli, E. A. Johnson, and M. Burt. I would also like to thank M. F. H. Schuurmans and R. Eppenga for some clarifications of the model in Refs. 12 and 40. I gratefully acknowledge financial support from Trinity College, Cambridge.

APPENDIX

We here derive an expression for the current density in the nonparabolic case and relate it to the boundary conditions at an interface. The Hamiltonian is written

$$H=-\frac{d}{dz}A\frac{d}{dz}+\frac{d^2}{dz^2}\alpha_0\frac{d^2}{dz^2}\ . \tag{A1}$$

Here A is the coefficient of the second-order term in k_z, which in the general case is

$$A=\frac{\hbar^2}{2m}+(2\alpha_0+\beta_0)k_{\parallel}^2\ . \tag{A2}$$

The effective mass and the nonparabolicity parameters α_0 and β_0 are z dependent and equal to m_1, α_{01}, and β_{01} in the quantum well and m_2, α_{02}, and β_{02} in the barriers. The expression for the current density j is derived from the continuity equation

$$\frac{d\rho}{dt}+\frac{dj}{dz}=0\ , \tag{A3}$$

where $\rho=F^*F$ is the charge density. Using the time-dependent Schrödinger equation and its complex conjugate we find

$$\frac{d\rho}{dt}=F^*\frac{dF}{dt}+F\frac{dF^*}{dt}=\frac{1}{i\hbar}(F^*HF-FHF^*)\ , \tag{A4}$$

and we obtain in the present case

$$\frac{dj}{dz}=\frac{1}{i\hbar}\left[\left[F^*A\frac{d^2F}{dz^2}-F^*\alpha_0\frac{d^4F}{dz^4}\right]-\text{c.c.}\right]\ , \tag{A5}$$

where c.c. stands for the complex conjugate of the first two terms. We want to evaluate the current density in the bulk materials some distance away from the interface so we do not need to include the derivatives of A and α_0.

It is seen that Eq. (A5) is fulfilled if

$$j=\frac{1}{i\hbar}\left[\left[F^*A\frac{dF}{dz}-F^*\alpha_0\frac{d^3F}{dz^3}+\frac{dF^*}{dz}\alpha_0\frac{d^2F}{dz^2}\right]-\text{c.c.}\right]. \tag{A6}$$

Note that we need the third term to avoid a term proportional to $dF^*/dz\, d^3F/dz^3$ in dj/dz. For the quantum-well case the current density is zero because the wave functions are real. However, the boundary conditions at an interface should be independent of the type of structure. We, therefore, consider a potential step at $z=0$ with an incoming wave, a reflected wave, and a transmitted wave:

$$F(z)=\begin{cases} I\exp(ik_1z)+R\exp(-ik_1z), & z<0 \\ T\exp(ik_2z), & z>0\ . \end{cases} \tag{A7a}$$

(A7b)

Here k_1 is given by (5) and k_2 by a similar expression with E replaced by $(E-V)$. The energy is taken to be larger than the size of the potential step V. Inserting this into (A6) we obtain

$$j=\begin{cases} j_1=\dfrac{2k_1}{\hbar}(A_1+2\alpha_{01}k_1^2)(|I|^2-|R|^2), & z<0 \quad \text{(A8a)} \\ j_2=\dfrac{2k_2}{\hbar}(A_2+2\alpha_{02}k_2^2)|T|^2, & z>0\ . \quad \text{(A8b)} \end{cases}$$

We want to see if different boundary conditions are consistent with current conservation, that is, the condition $j_1=j_2$. If we assume that the boundary conditions at an interface are given by the continuity of the envelope function F and

$$A\frac{dF}{dz}-\alpha_0\frac{d^3F}{dz^3} \tag{A9}$$

[cf. Eq (17) and Ref. 16] we can express the amplitude of the reflected wave and the transmitted wave in terms of that of the incoming wave. We obtain

$$\frac{R}{I}=\frac{A_1k_1+\alpha_{01}k_1^3-A_2k_2-\alpha_{02}k_2^3}{A_1k_1+\alpha_{01}k_1^3+A_2k_2+\alpha_{02}k_2^3}, \tag{A10}$$

$$\frac{T}{I}=\frac{2(A_1k_1+\alpha_{01}k_1^3)}{A_1k_1+\alpha_{01}k_1^3+A_2k_2+\alpha_{02}k_2^3}. \tag{A11}$$

Insertion into (A8) does not give $j_1=j_2$. If $2\alpha_0$ had been replaced by α_0 in (A8a) and (A8b), which corresponds to the usual expression for j but with the mass given by the perpendicular mass [Eq. (9)], we would have obtained $j_1=j_2$. In the present case it is readily verified that current conservation is fulfilled if α_0 is replaced by $2\alpha_0$ in Eqs. (A10) and (A11). We thus find that continuity of F and

$$A\frac{dF}{dz}-2\alpha_0\frac{d^3F}{dz^3} \tag{A12}$$

is compatible with conservation of the current density. When this is applied to the quantum-well case, we obtain Eq. (18) with $N=2$.

*Present address.

[1]E. O. Kane, J. Phys. Chem. Solids **1**, 249 (1957).

[2]G. Bastard, Phys. Rev. B **24**, 5693 (1981); **25**, 7584 (1982).

[3]G. Bastard, in *Molecular Beam Epitaxy and Heterostructures*, edited by L. L. Chang and K. Ploog (Martinus Nijhoff, Dordrecht, 1985), p. 381.

[4]S. Yamada, A. Taguchi, and A. Sugimura, Appl. Phys. Lett. **46**, 675 (1985).

[5]U. Rössler, Solid State Commun. **49**, 943 (1984).

[6]F. Malcher, G. Lommer, and U. Rössler, Superlatt. Microstruct. **2**, 267 (1986).

[7]R. Lassnig, Phys. Rev. B **31**, 8076 (1985).

[8]U. Ekenberg, in *Proceedings of the 19th International Conference on the Physics of Semiconductors* (Polish Academy of Sciences, Warsaw, 1988), p. 287.

[9]U. Ekenberg, Phys. Rev. B **36**, 6152 (1987).

[10]M. Braun and U. Rössler, J. Phys. C **18**, 3365 (1985).

[11]J. M. Luttinger and W. Kohn, Phys. Rev. **97**, 869 (1955).

[12]M. F. H. Schuurmans and G. W. 't Hooft, Phys. Rev. B **31**, 8041 (1985).

[13]D. L. Smith and C. Mailhiot, Phys. Rev. B **33**, 8345 (1986); C. Mailhiot and D. L. Smith, *ibid.* **33**, 8360 (1986).

[14]D. J. BenDaniel and C. B. Duke, Phys. Rev. **152**, 683 (1966).

[15]M. G. Burt, Semicond. Sci. Technol. **2**, 460 (1987); **2**, 701(E) (1987); **3**, 739 (1988); **3**, 1224 (1988).

[16]M. de Dios Leyva, J. López Gondar, and J. Sabín del Valle, Phys. Status Solidi B **142**, K151 (1987); **145**, K155(E) (1988).

[17]C. Priester, G. Bastard, G. Allan, and M. Lannoo, Phys. Rev. B **30**, 6029 (1984).

[18]E. A. Johnson and A. MacKinnon, J. Phys. C **21**, 3091 (1988).

[19]G. Lommer, F. Malcher, and U. Rössler, Superlatt. Microstruct. **2**, 273 (1986).

[20]See, e.g., Fig. 2 in E. Finkman, M. D. Sturge, M.-H. Meynadier, R. E. Nahory, M. C. Tamargo, D. M. Hwang, and C. C. Chang, J. Lumin. **39**, 57 (1987).

[21]J. Singleton, R. J. Nicholas, D. C. Rogers, and C. T. B. Foxon, Surf. Sci. **196**, 489 (1988).

[22]T. Duffield, R. Bhat, M. Koza, F. DeRosa, D. M. Hwang, P. Grabbe, and S. J. Allen, Jr., Phys. Rev. Lett. **56**, 2724 (1986).

[23]F. Ancilotto, A. Fasolino, and J. C. Maan, Superlatt. Microstruct. **3**, 187 (1987).

[24]See, e.g., F. M. Peeters, X. Wu, and J. T. Devreese, Phys. Rev. B **37**, 933 (1988), and references therein.

[25]D. F. Welch, G. W. Wicks, and L. F. Eastman, J. Appl. Phys. **55**, 3176 (1984).

[26]T. Hiroshima and R. Lang, Appl. Phys. Lett. **49**, 456 (1986).

[27]D. F. Nelson, R. C. Miller, and D. A. Kleinman, Phys. Rev. B **35**, 7770 (1987).

[28]A. Persson and R. M. Cohen, Phys. Rev. B **38**, 5568 (1988).

[29]The parameter γ used in Ref. 27 is defined by the relation $E=\hbar^2k^2(1-\gamma k^2)/(2m)$ and its relations to the parameters used in this article are $\gamma=\alpha'\hbar^2/(2m)$ and $\gamma=-2m\alpha_0/\hbar^2$.

[30]In Ref. 28 the dispersion is written $E=a_2p^2-a_4p^4$, where $a_2=(2m)^{-1}$ and $a_4=(2m)^{-2}\alpha'=-\hbar^{-4}\alpha_0$ in the notation

used in the present article.
[31]J. R. Chelikowsky and M. L. Cohen, Phys. Rev. B **14**, 556 (1976).
[32]R. L. Kolbas, Ph.D. thesis, University of Illinois at Urbana-Champaign, 1979 (unpublished); B. A. Vojak, W. D. Laidig, N. Holonyak, Jr., M. D. Camras, J. J. Coleman, and P. D. Dapkus, J. Appl. Phys. **52**, 621 (1981).
[33]M. Cardona, Phys. Rev. **121**, 752 (1961).
[34]L. G. Shantarama, A. R. Adams, C. N. Ahmad, and R. J. Nicholas, J. Phys. C **17**, 4429 (1984). The parameter determined in this paper, $E_p=25$ eV, corresponds to $2m_0P^2$ in the notation of Ref. 3.
[35]H. C. Casey, Jr., and M. B. Panish, *Heterostructure Lasers* (Academic, New York, 1978).
[36]M. Zachau, F. Koch, G. Weimann, and W. Schlapp, Phys. Rev. B **33**, 8564 (1986).
[37]In Ref. 3, it was claimed that the ground-state energy is lower in the nonparabolic case if this procedure is followed. The reason for this discrepancy is not understood.
[38]Note that a different notation was used in Refs. 2 and 3. There $\mathbf{k}_\perp$ was used for the wave vector parallel to the layers, i.e., perpendicular to the growth direction.
[39]J. M. Luttinger, Phys. Rev. **102**, 1030 (1956).
[40]R. Eppenga, M. F. H. Schuurmans, and S. Colak, Phys. Rev. B **36**, 1554 (1987).
[41]N. F. Johnson, H. Ehrenreich, K. C. Hass, and T. C. McGill, Phys. Rev. Lett. **59**, 2352 (1987).
[42]L. D. L. Brown, M. Jaros, and D. Ninno, Phys. Rev. B **36**, 2935 (1987).
[43]U. Ekenberg and M. Altarelli, Phys. Rev. B **35**, 7585 (1987).